Journal of Sustainability Science and Management
Volume 15 *Number* 7, October 2020: 83-101
eISSN: 2672-7226

ANALYTICAL SOLUTION OF A MATHEMATICAL MODEL TO SIMULATE NITRITE POLLUTANT TRANSPORT ALONG A RIVER

OLOWE KAYODE O*[1] AND MUTHUKRISHNAVELLAISAMY KUMARASAMY[2]

[1]Civil Engineering department, Afe-Babalola University, Ado-Ekiti, Nigeria. [2]Civil Engineering Programme, School of Engineering, University of KwaZulu-Natal, Durban, South Africa.

**Corresponding author: owenkaay2001@yahoo.com*
Submitted final draft: 22 March 2020 *Accepted: 30 April 2020* http://doi.org/10.46754/jssm.2020.10.009

Abstract: This research focuses on developing a mathematical model to simulate the spatial and temporal variations of nitrite concentration in a natural river. A conceptual hybrid cell in series model (HCIS-NO_2) was developed for a first-order kinetic reaction of nitrite, along with the advection and dispersion processes, using the mass balance concept. The proposed model considers the transformation of nitrite to nitrate and the oxidation of ammonia to nitrite due to the nitrification process. An analytical solution of the HCIS-NO_2 model was obtained using Laplace transformation. It was observed that the new model's responses agreed with the advection-dispersion equation model coupled with nitrite kinetics (ADE-NO_2). An explicit finite difference scheme was used to solve ADE-NO_2 for demonstration purposes. The nitrite concentration simulation obtained from the proposed model is in good agreement with the data collected from Umgeni River in South Africa. The simulated concentration profiles along the river reach matched closely with the measured data, which can be noted from the coefficient of determination (R^2) value of 0.76 and a low standard error (SE). The study shows that the development of this model is useful for the prediction of nitrite pollutant concentration in a natural river.

Keywords: Nitrite nutrients, mathematical model, hybrid cells model, Umgeni River.

Introduction

The increase in pollution caused by industrialisation, urbanisation, and agriculture has impacted the health of river ecosystems. Various studies have shown that one of the primary pollutant threats to river health is the high influx of nutrients in rivers (Nyenje *et al*., 2010; Varol & Sen, 2012; Kiedrzyńska *et al*., 2014; Gavrilescu *et al*., 2015). Eutrophication occurs when a surface water is enriched with a high quantity of nutrients that stimulate algae growth, which results in the decrease of dissolved oxygen (DO) concentration (Smith & Schindler, 2009; Lewis *et al*., 2011; Zamparas & Zacharias, 2014), prompting a further decline in water quality. The adequate evaluation of DO and nutrients in a water column is essential for the existence of aquatic habitats and the health of an aquatic ecosystem. Hence, it is necessary to evaluate some of the nutrients being discharged into a surface water (Peredes *et al*., 2010; Kannel *et al*., 2011). Nitrite nutrients are one of the critical parameters in determining a water body's suitability for drinking purposes and for use by aquatic animals. Nitrites mostly form due to the oxidation of ammonia in water bodies, and they can come from other sources, which include fertilisers, animal waste, and human waste discharged into the rivers and streams (Raimonet *et al*., 2015). Liu *et al*. (2005) describe the nitrification of ammonia as a two-step biochemical process through which ammonia is reduced to nitrite and then nitrite is converted to nitrate. Most of the potential health effects of nitrites are seen in infants between the ages of 0-6 months, which manifests as a temporary blood disorder called methaemoglobinaemia (Samatya *et al*., 2006).

Restoring the quality of water bodies to an acceptable level requires effective management of these pollutants through rigorous water quality monitoring and modelling. The application of different water quality modelling (WQM) tools is often demonstrated as an effective and cost-efficient method for water quality assessment. Different WQM tools have

been applied in many studies to determine the effect of nutrient pollutants transport in surface water. Yuceer *et al.* (2016) used a continuous stirred tank reactor (CSTR) method to simulate water quality constituents, which include nitrite concentration, in Beylerderesi River in Turkey. They applied the optimisation technique to estimate the model parameters by using the sequential Quadratic programming (SQP) method. Their results agreed with the measured data of nitrite concentration in the water body. Oliveira *et al.* (2012) discovered significant nutrient enrichment in Certima River in Portugal by using the QUAL2KW model to evaluate the response of different loads of nutrients in the river. They identified domestic and diffuse sources of contamination as the main sources of nitrogen nutrient in the river. The model adequately described the measured data of nutrients satisfactorily. Silva *et al*. (2015) used a statistical analysis to assess the temporal and spatial distributions of nitrite concentration in Cachoeira River in Brazil, where a low concentration of nitrite was detected. Vonder Wiesche *et al*. (1998) highlighted how environmental factors and inorganic nitrogen affect the variation of nitrite concentration in Lahn River in Germany. They stated that the increase in nitrite concentration in the river was due to the high water temperature and high level of ammonia concentration. Corriveau *et al*. (2010) reported the effect of an agricultural watershed on the influx of nutrients in Brasdhenri River in Quebec. They observed that there was an increase in nitrite concentration in the river during the summer period, with a low flow. Mirbagheri *et al*. (2009) developed a model to evaluate parameters such as DO, BOD, ammonia, nitrites, and nitrates in Jajrood River in Iran. They used an implicit finite difference scheme to solve their model equations. The results obtained from their model were able to describe the parameters in the river effectively. Wang *et al*. (2011) presented an application of the MIKE II model on the effects of nutrients transport in the lower and middle reaches of Hanshui River. They developed a rainfall-runoff model to estimate the amount of nutrient pollutant discharged into the river from the catchment. The results of their study showed a good simulation of the river nutrients when compared with the observed data.

Different methods were used to solve solute transport in a water body, which includes the finite difference scheme and analytical methods. The Fickian-based ADE equation was numerically solved using the finite difference scheme and has been a popular method for solving pollutants transport in rivers and streams. In using the ADE method, whether in its analytical form or numerical scheme, the accurate estimation of flow (u) and longitudinal dispersion coefficient (D_L) is important. The flow can be estimated quite easily and accurately by employing gauged flows or by using a flow resistance equation. However, the estimation of the dispersion coefficient (D_L) is not straightforward. The compilation works of many investigators (Seo & Cheong, 1998; Etemad-Shahidi & Taghipour, 2012; Sattar & Gharabaghi, 2015; Balf *et al.,* 2018; Seifi & Riahi-Madvar, 2019) reported a wide range of D_L values that have been estimated either by theoretical or experimental bases, or by empirical formulae. The process of determining the D_L adopted in this study was the empirical method developed by Etemad-Shahidi and Taghipour (2012). These equations depend on the fluid properties, channel geometrics and hydraulic characteristics of the reaches. It is a significant parameter in estimating the distribution of solute concentration in a natural water body. The ADE model has its limits, in which it is ineffective in practical applications (Ghosh *et al*., 2008; Neuman & Tartakovsky, 2009). The cell-in-series (CIS) model was developed to serve as an alternative to the ADE model sin terms of simulating pollutant transport in a water body (Banks, 1974; Wang & Chen, 1996). However, the CIS model cannot simulate the advection component effectively, where the river reach is assumed to be a thoroughly mixed cell (Kumarasamy, 2015). The HCIS model was developed to solve solute pollutant transports in surface water and to resolve the limitations associated with the existing models (Kumarasamy *et al.,* 2011). The new model

applied an ordinary differential equation that can be analytically solved, which makes it advantageous over the ADE model. Additionally, the ability to simulate the advection component with the new model tackles the limitation of the CIS model (Kumarasamy *et al.,* 2013).

Thus, the HCIS model has been demonstrated to have some merit over the previous models as described by Ghosh *et al.* (2004). The model equation is a first-order ordinary differential equation that can be solved analytically. Also, the model could describe the advection component of solute transport due to the introduction of a plug flow zone. The inclusion of the plug flow zone has allowed for the estimation of the first arrival time of a pollutant in a river reach. Furthermore, it can incorporate additional solute kinetic reactions to its three compartments, and the resulting equation would be solved analytically. The model has been able to demonstrate its ability to simulate solute transport in natural water. The main contribution of this research is to use the HCIS model as an alternative model for solute transport studies in natural streams and, consequently, it is a motive for this present study. In this study, an analytical solution was developed for the HCIS model, which incorporates the first-order kinetic reaction of nitrite, coupled with the ADE processes for simulating the spatial and temporal variations of nitrite pollutant in natural rivers. The developed HCIS-NO_2 model was used to evaluate the nitrite concentration of Umgeni River. This study also illustrates the numerical solution for a Fickian-based ADE model, coupled with the first-order reaction of nitrite processes. The results of both models were compared.

Methodology

A river reach is divided into a series of conceptual hybrid units. Each hybrid unit is assumed to consist of a plug cell and two thoroughly mixed cells as presented in Figure 1. The first cell has a residence time (T_1), and the other two cells have unequal residence times (T_2 and T_3), all of which are the model parameters. The concentrations of nitrite pollutant C_b (x, t) vary with time (t) along the length of the river reach, which is affected by a point-source pollutant. The conversion of ammonia to nitrite through the action of the *Nitrosomona* bacteria, and agricultural and industrial wastes were assumed to be the sources of nitrite in the water column. The oxidation of nitrite to nitrate through the action of the *Nitrobacter* bacteria was considered as a sink of nitrite in the river system.

Sakalauskienė (2001) presented the first-order kinetic equation of nitrite as expressed in Eq. (1).

$$\frac{\partial C_b(x,t)}{\partial t} = k_a C_a(x,t) - k_b C_b(x,t) \quad (1)$$

Where C_a represents the ammonia concentration in the river (mg/l), (k_a) represents the oxidation rate of ammonia (day-^{1}), C_b is the nitrite concentration (mg/l) and k_b is the rate of production of nitrite to nitrate (day-1). In addition, (x) could be described as the distance

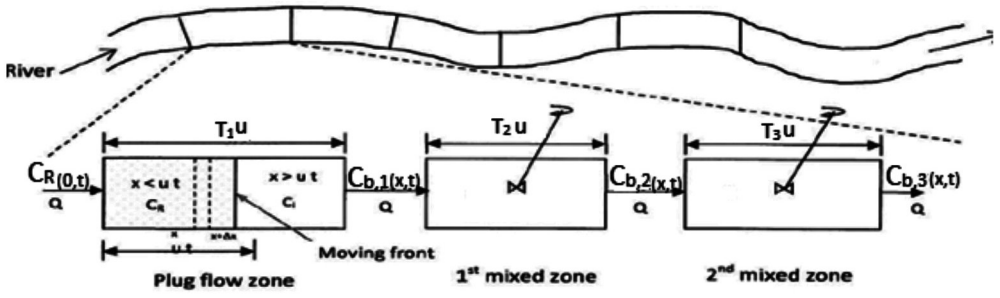

Figure 1: The conceptual unit of hybrid cells in the series model

along the river from the point of injection of the pollutant (m) and (t) is the time required for the pollutant to move from one point to another in the river reach (min). From Eq. (1), the first term on the right side defines the process by which nitrite is generated through the oxidation of ammonia, and the second term describes the way through which nitrite is removed through biochemical oxidation to nitrate.

The process of the HCIS model begins in the plug flow cell, where the nitrite concentration undergoes a pure transformation without a variation in concentration. The effluents from the first cell enter the second cell, where they get thoroughly mixed for a period before they enter the third cell. Thus, it can be concluded that the transport of nitrite solute in the first cell signifies pure advection. Moreover, the advection-dispersion process takes in the two mixing cells. We assumed that the original concentration of nitrite solute in the entire cell is zero and the boundary concentration changes from 0 to C_R. The nitrification of ammonia to nitrite concentration and decay of nitrite concentration to nitrate occur in all the three cells as the nitrite pollutant travels downstream. We considered the flow rate Q (m^3/s) for the river flow to be in a steady condition. In this study, the HCIS model will be used to predict the nitrite concentration in the river reach using Laplace transformation, mass balance and convolution at the end of successive units.

Formulation of Nitrite Concentration in the Plug Flow Cell

A plug flow cell was assumed to have control volume (V) and length (Δx), and was considered to transport a concentration of nitrite pollutant C_b (x, t) downstream. The plug flow cell consists of a compartment that contains a plume of water. T_1 is the time required for the fluid to stay in the plug flow cell before it gets replaced. A little time interval (Δt) was considered, where some portion of the nitrite (NO_2) pollutant concentration is transformed into nitrate (NO_3). Also, the ammonia (NH_3) concentration is converted to nitrite during the oxidation process within the system. After the nitrification and oxidation processes, the nitrite solute in the river will move to the next control volume. The following partial differential equation was formulated as expressed in Eq. (2).

$$\frac{\partial C_b(x,t)}{\partial t} + \frac{u\partial C_b(x,t)}{\partial x} = k_a C_a(x,t) - k_b C_b(x,t) \quad (2)$$

Eq. (2) was solved using the following initial and boundary conditions, which are C_b (x, 0) = 0 for x > 0; C_b (0, t) = C_R for t ≥ 0; C_b (T_1u, t) = 0 for 0 < t < T_1. The nitrite pollutant concentration at the inlet boundary is represented as C_R.

Eq. (2) was solved using Laplace transformation, integration and inverse Laplace transformation to obtain

$$C_{b,1}(x,t) = \left[C_R U(t-T_1)e^{-k_b T_1}\right] + \left[\frac{k_a C_{a,1}(x,t)}{k_b}\left\{e^{-k_b t} - U(t-T_1)e^{-k_b T_1}e^{-k_b(t-T_1)}\right\}\right] \quad (3)$$

The nitrite concentration at the end of the plug flow cell was presented in Eq. (3) and is valid for t ≥ T_1, where U (t – T_1) is a step function and $C_{a,1}$(x, t) is the concentration of ammonia in the plug flow cell (Olowe and Kumarasamy 2017).

Formulation of Nitrite Concentration in the First Well-Mixed Cell

The nitrite concentration at the end of the first cell will be the input of the first thoroughly mixed cell after moving through the plug flow cell length T_1u. The residence time required for the first thoroughly mixed cell is $T_2 = V_2/Q$, where V_2 is the volume of the first mixed cell and Q is the flow rate of the cell. The mass balance of the concentration of nitrite pollutant in the second cell is presented in Eq. (4)

$$C_{b,1}Q\Delta t - C_{b,2}Q\Delta t + k_a C_{a,2}V_2\Delta t - k_b C_{b,2}V_2\Delta t = V_2\Delta C_{b,2} \quad (4)$$

The first and second terms on the left-hand side indicates the mass of nitrite concentration pollutant entering and leaving the first mixed cell. The third term represents the conversion of ammonia to nitrite, and the last term represents the biochemical oxidation of nitrite to nitrate concentration in the river. The right term describes the change of mass within the first mixed cell. Eq. (4) was described in the ordinary differential form, which was solved to give the concentration of nitrite pollutant at the end of the cell.

Formulation of Nitrite Concentration in the Second Well-Mixed Cell.

The cell was considered to have a residence time $T_3 = V_3/Q$. The nitrite pollutant from the first mixing cell will move to the second mixing cell. In the cell, the nitrite concentration will decay to nitrate pollutant and the accumulation of nitrite due to the nitrification of ammonia concentration will occur. Therefore, the equation below represents the mass balance in the cell.

$$C_{b,2}Q\Delta t - C_{b,3}Q\Delta t + k_a C_{a,3}V_3\Delta t - k_b C_{b,3}V_3\Delta t = V_3\Delta C_{b,3} \quad (5)$$

The first and second terms on the left-hand side indicates the mass of nitrite concentration pollutant entering and leaving the second mixed cell. The third term represents the conversion of ammonia to nitrite and the last term represents the biochemical oxidation of nitrite to nitrate concentration in the river. The right term describes the change of mass within the second mixed cell. Eq. (5) was expressed as a first-order differential form and resolved to estimate the step response function of the concentration of nitrite at the end of the hybrid unit as:

$$C_{b,3} = \left[\begin{array}{l} \left(\dfrac{C_R U(t-T_1)}{(1+k_bT_2)(1+k_bT_3)}\{A\}\right) - \left(\dfrac{C_R U(t-T_1)T_2 e^{-k_bT_2}}{(1+k_bT_2)(T_2-T_3+k_bT_2T_3)}\{B\}\right) \\ + \left(\dfrac{k_aC_{a,1}}{k_b}\{D\} - \dfrac{k_aC_{a,1}U(t-T_1)}{k_b}\{N\}\right) + \left(\dfrac{T_2k_aC_{a,2}}{(1+k_bT_2)}\{\Phi\} + \dfrac{T_3k_aC_{a,3}}{(1+k_bT_3)}\{\Omega\}\right) \end{array}\right] \quad (6)$$

where

$$A = \left\{\left(e^{-k_bT_1}\right) - \left(e^{\left(1/T_3\right)[T_1-t]}e^{-k_bt}\right)\right\},\ B = \left\{\left(e^{\left(1/T_2\right)[T_1-t]}\right) - \left(e^{\left(\frac{1+k_bT_3}{T_3}\right)[T_1-t]}\right)\right\}$$

$$\mathrm{N} = \left\{\begin{array}{l} \left(\dfrac{e^{k_bt}}{(2T_3k_b+1)}\right) - \left(\dfrac{T_2e^{\left(1/T_2\right)T_1}e^{-\left(\frac{1+k_bT_2}{T_2}\right)t}}{(T_2-T_3)}\right) \\ - \left(\dfrac{e^{k_bT_1}e^{\left(\frac{1+k_bT_3}{T_3}\right)(T_1-t)}}{(2T_3k_b+1)}\right) + \left(\dfrac{T_2e^{\left(1/T_3\right)T_1}e^{-\left(\frac{1+k_bT_3}{T3}\right)t}}{(T_2-T_3)}\right) \end{array}\right\}$$

$$D=\left\{\begin{array}{l}\left(\dfrac{e^{k_b t}}{\left(2T_3k_b+1\right)}\right)-\left(\dfrac{T_2e^{\left(1/T_2\right)T_1}e^{-\left(\frac{1+k_bT_2}{T_2}\right)t}}{\left(T_2-T_3\right)}\right)\\ -\left(\dfrac{e^{k_bT_1}e^{\left(\frac{1+k_bT_3}{T_3}\right)\left(T_1-t\right)}}{\left(2T_3k_b+1\right)}\right)+\left(\dfrac{T_2e^{\left(1/T_3\right)T_1}e^{-\left(\frac{1+k_bT_3}{T_3}\right)t}}{\left(T_2-T_3\right)}\right)\end{array}\right\}$$

$$\Phi=\left\{\begin{array}{l}\left(\dfrac{1}{\left(1+k_bT_3\right)}\right)-\left(\dfrac{T_2e^{\left(\frac{1+k_bT_2}{T_2}\right)\left(T_1-t\right)}}{\left(T_2-T_3\right)}\right)\\ -\left(\dfrac{e^{\left(\frac{1+k_bT_3}{T_3}\right)\left(T_1-t\right)}}{\left(1+k_bT_3\right)}\right)+\left(\dfrac{T_2e^{\left(\frac{1+k_bT_3}{T_3}\right)\left(T_1-t\right)}}{\left(T_2-T_3\right)}\right)\end{array}\right\},\ \Omega=\left\{1-e^{\left(\frac{1+k_bT_3}{T_3}\right)\left(T_1-t\right)}\right\}$$

Eq. (6) simulates the concentration of nitrite at the end of the first hybrid unit and represents the step response of the first hybrid unit, where $C_{b,3}$ [mg/l] is the concentration of the nitrite solute at the end of the second thoroughly mixed cell; and, $C_{a,2}$ and $C_{a,3}$ (mg/l) simulates the concentration of ammonia in both mixed cell, respectively. The impulse response function $d_{HCIS\text{-}NO2}$ (n, Dt) was estimated numerically by differentiating the step response function with respect to (t) as shown below:

Where $K_{HCIS-NO2}$ is the step response of the first hybrid unit, which is equivalent to $C_{b,3}$. Eqs. (6) and (7) are valid for $t \geq T_1$ and represent the unit step and the unit impulse response functions of a hybrid unit. Eq. (8) presents a convolution technique to determine the nitrite concentration at the downstream location along the river. The process considers a river as a series of hybrid units where the concentration of nitrite pollutant from one hybrid unit will be the influent to the next unit as presented in Figure 2.

$$\delta_{HCIS-NO_2}\left(n,\Delta t\right)=\frac{K_{HCIS-NO_2}\left(n\Delta t\right)-K_{HCIS-NO2}\left(\left(n-1\right)\Delta t\right)}{\Delta t} \tag{7}$$

$$C\left(i\Delta x,n\Delta t\right)=\sum_{\gamma=1}^{n}C\left[\left(i-1\right)\Delta x,\gamma\right]\delta_{HCIS-NO_3}\left(n-\gamma+1,\Delta t\right) \tag{8}$$

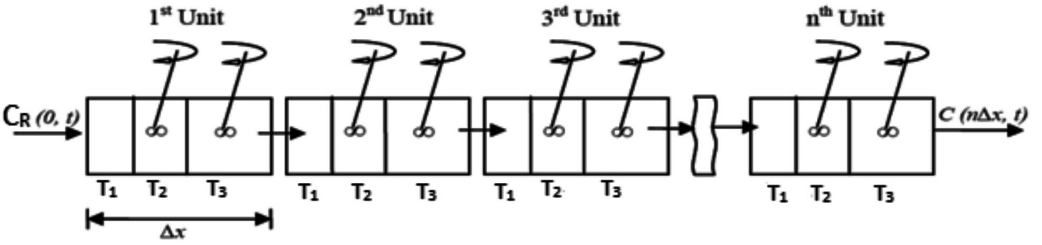

Figure 2: A composed series of hybrid units representing a stream reach with length nΔx

Model Parameters

The model parameters T_1,T_2 and T_3, which are the residence times of pollutant in the hybrid units of the proposed model, can be determined (Ghosh, 2001; Ghosh et al., 2008). It has been estimated that the parameters satisfy the Peclet number $P_e = \Delta x u / D_L$ ³ 4. The model parameters depend on the dispersion coefficient and the size of the hybrid unit, which are calculated as: $T_1 = 0.04\ \Delta x^2 / D_L$, $T_2 = 0.05\ \Delta x^2 / D_L$ *and* $T_3 = (\Delta x / u) - (0.09\ \Delta x^2 / D_L)$.

Comparison of the HCIS-NO_2 Model with the ADE- NO_2 Model

The capability of the HCIS-NO_2 model was verified by comparing it with a Fickian-based ADE-NO_2 model. The partial differential equation of the ADE equation, along with first-order reaction of nitrite for a one-dimensional flow, is given as:

Where C_b [mg/l] is the nitrite concentration; C_a [mg/l] is the ammonia concentration; K_b [day-^{1}] is the rate constant for the oxidation of nitrite, which is temperature-dependent; and, Ka [day-^{1}] is the rate of oxidation of ammonia.

The initial and boundary conditions used for Eq. (2) were used to solve Eq. (9) by applying an explicit finite difference scheme. The process considered the forward difference in time, the central difference in space for the dispersion term, and backward upwind for the advection term, which yields the solution described in Eq. (10) and the result was compared with the HCIS-NO_2 model. A small courant number was used, which must be less than or equal to 1 for the numerical solution to be accurate and stable. The time step and grid space were chosen as Δt = 1min and Δx =100m, respectively

$$\frac{\partial C_b(x,t)}{\partial t} = -u\frac{\partial C_b(x,t)}{\partial x} + D_L\frac{\partial^2 C_b(x,t)}{\partial x} + k_a C_a(x,t) - k_b C_b(x,t) \tag{9}$$

$$C(x,t+\Delta t) = \left[\begin{array}{l} \left(C(x,t)\left[1-\frac{2D_L\Delta t}{(\Delta x)^2}-k_b\Delta t\right]\right)-\left(C(x+\Delta x,t)\left[\frac{u\Delta t}{2\Delta x}-\frac{D_L\Delta t}{(\Delta x)^2}\right]\right) \\ +\left(C(x-\Delta x,t)\left[\frac{u\Delta t}{2\Delta x}+\frac{D_L\Delta t}{(\Delta x)^2}\right]\right)+C_a(x,t)(k_a\Delta t) \end{array}\right] \tag{10}$$

Results and Discussions

Model Simulation and Testing

The spatial and temporal variations of nitrite concentration in a river were simulated to demonstrate the potential of the new model, where a synthetic dataset was generated for the river. The parameters T_1, T_2, and T_3 of the HCIS-NO_2 model were estimated as T_1 = 1.70 min, T_2 = 2.30 min and T_3 = 6.0 min by considering a river with anticipated values for u and D_L. The value of u and D_L were given as 20m/min and 1000m^2/min, respectively, and the size of the hybrid unit Δx = 200m was determined by satisfying the Peclet number condition. The transformation of NH_3 to NO_2 and the conversion of NO_2 to NO_3 concentration through the nitrification process were considered in the proposed model. Considering the estimated model parameters (T_1, T_2, and T_3) and different values of k_b (= 0.002 and 0.005 per min), the unit step and impulse response functions of the first hybrid unit as computed using Eqs. (6) and (7) are presented in Figure 3 and 4. Figure 3 shows the step response of the nitrite concentration with respect to time for different oxidation rate of nitrite k_b (= 0.002 and 0.005 per min), while the NH_3 oxidation rate (k_a) was kept constant. It can be seen from the figure that there was an increase in the concentration of nitrite as time increases until it reaches the boundary concentration. In addition, it was observed that the effluent of the lower k_b value attains the boundary concentration earlier than the effluent from the higher k_b value. The impulse response described in Figure 4 shows that there was a reduction in the peak concentration and the recession limb extended for a long time with the increase in k_b value in the water body. Thus, the variation in the nitrification rate (k_b) affects the nitrite pollutants as it moves downstream and makes it more attenuated within the water body.

The impulse response functions were generated at the end of the 1st, 2nd, 4th and 8th hybrid units using the nitrite oxidation rates k_b (= 0.002 and 0.005per min) while the ammonia oxidation rate (k_a) was kept constant as shown in Figure 5. It could be observed that as the nitrite pollutant moves downstream, the C-t distribution gets more attenuated and the peak concentration reduces as the hybrid units increase. Furthermore, the time to peak reduces as the hybrid units increase. Therefore, it can be observed that the reduction in nitrite pollutant as it travels downstream in the river was due to the nitrification process, which converts nitrite to nitrate concentration.

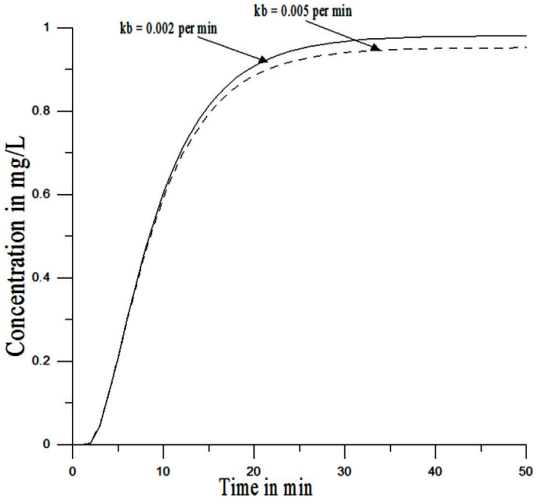

Figure 3: The unit step responses of the HCIS-NO_2 model, with nitrification rate co-efficient k_b= 0.002 per min and 0.005 per min at the end of first hybrid unit for T_1 = 1.7 min, T_2 = 2.3 min, T_3 = 6.0min, u = 20 m/min and Δx = 200 m

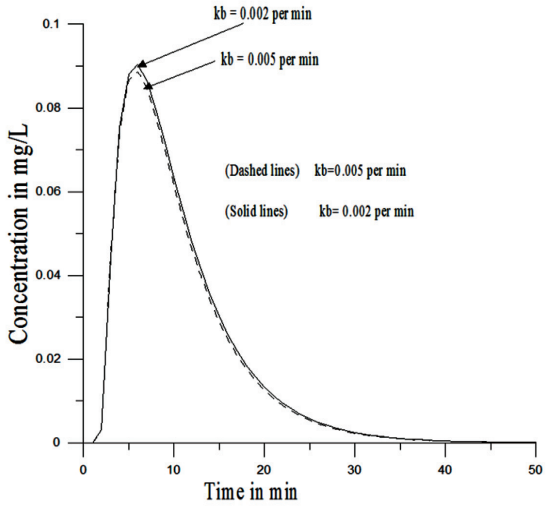

Figure 4: The unit impulse responses of the HCIS-NO_2 model, with nitrification rate co-efficient k_b = 0.002 per min and 0.005 per min at the end of first hybrid unit for T1 = 1.7 min, T 2 = 2.3 min, T3 = 6.0 min, u = 20 m/min and Δx = 200 m

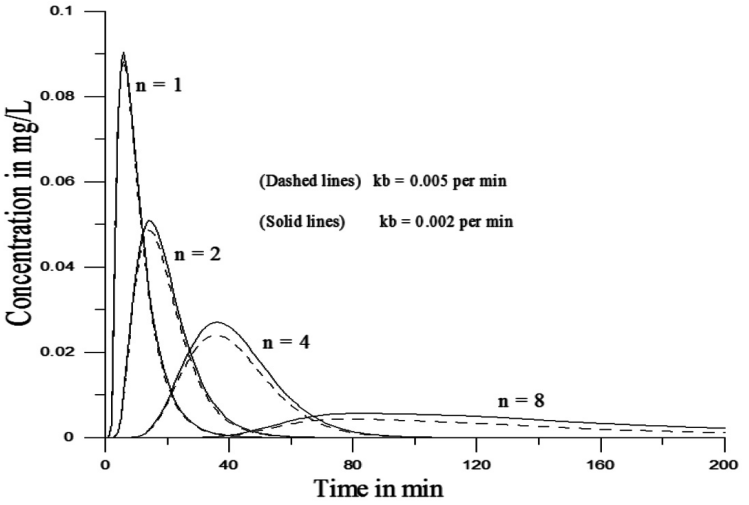

Figure 5: The unit impulse responses of the HCIS-NO_2 model, with nitrification rate co-efficient, k_b = 0.002 and 0.005 per min, at the end of the first (n = 1), second (n = 2), fourth (n = 4) and eighth (n = 8) hybrid units for T_1 = 1.7 min, T_2 = 2.3 min, T_3 = 6.0 min, u = 20 m/min and Δx = 200 m

Figure 6 was used to illustrate the effect of the ammonia oxidation rate on the variation of the concentration of nitrite pollutant as it travels downstream within the river, where values of k_a (=0.002 and 0.005 per min) were used while (k_b) was kept constant. It can be observed that the higher value of k_a leads to the increase in nitrite concentration in the river when compared with the lower value of k_a. In addition, a bell-shaped distribution was observed in the profile, and as the nitrite pollutant travels downstream, the peak concentration reduces and the falling limb is elongated as the number of units increase.

The performance of the new model was validated with the impulse response of the numerical solution of the Fickian-based ADE-

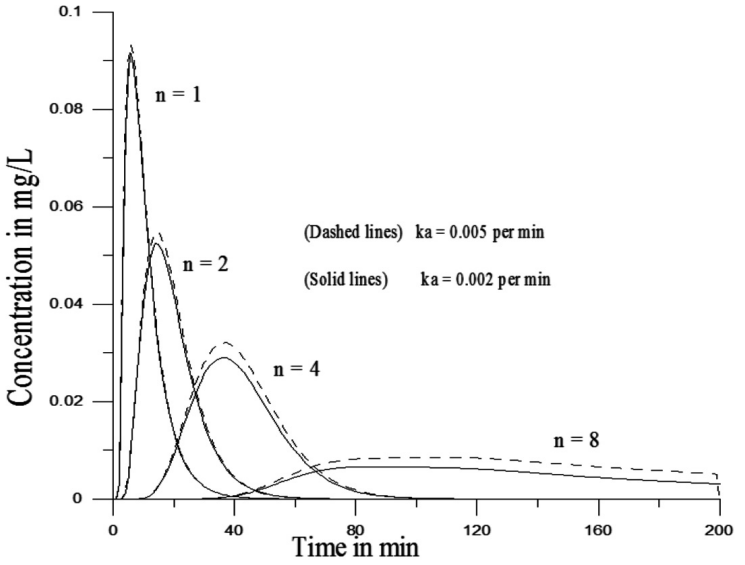

Figure 6: The unit impulse responses of the HCIS-NO_2 model, with ammonia oxidation decay rate co-efficient, k_a = 0.002 and 0.005 per min, at the end of the first (n = 1), second (n = 2), fourth (n = 4) and eighth (n = 8) hybrid units for T_1 = 1.7 min, T_2 = 2.3 min, T_3 = 6.0 min, u = 20 m/min and Δx = 200 m

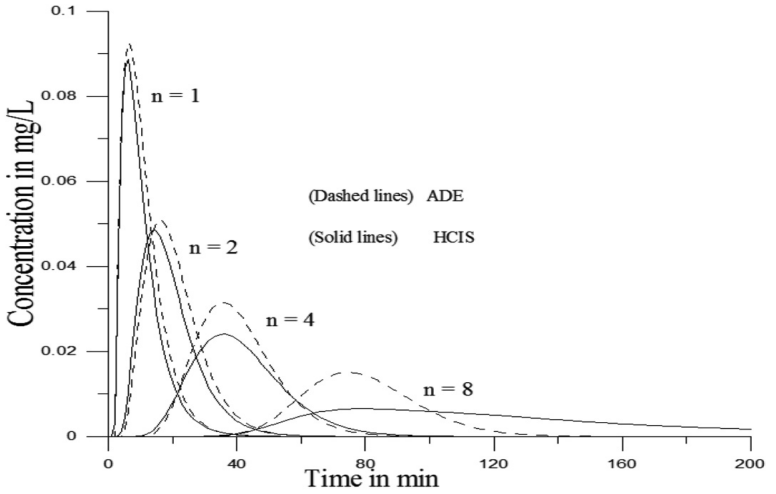

Figure 7: The unit pulse responses of the ADE model (u = 20 m/min; DL = 1000 m2/min and at 200, 400, 800 and 1600m) and the HCIS-NO_2 model at the end of the first (n = 1), second (n = 2), fourth (n = 4) and eighth (n = 8) hybrid units T1 =1.7 min; T2 = 2.3 min; T3 = 6.0 min; Δ x = 200 m, for nitrification rate co-efficient, k_b = 0.005 per min

NO_2 model as shown in Figure 7. Eq. (10) was numerically differentiated with respect to time to determine the impulse response of the ADE-NO_2 model. The following dataset was used for the simulation of the ADE-NO_2 model: Δt = 1min, Δx =100m, flow velocity (u) = 20m/min and dispersion coefficient D_L = 1000m^2/min. The impulse responses at the point when (X = 200m) and when (X = 400m, 800m and 1600m) from the point of injection are described in Figure 7. Numerical convolution was used to determine the concentration of nitrite

pollutant downstream. The impulse responses were generated at the same location at the end of the 1st, 2nd, 4th and 8th hybrid units as presented in Figure 7. It could be observed that the concentration-time profiles agreed with each other and show similar conditions as the nitrite pollutant moves downstream. Moreover, the peak and shape of the C-t profile was satisfactorily produced by both models. However, marginal differences in the peak concentration were observed in the profile due to the difference in space discretisation. Also, the truncation procedure followed in solving the ADE model using the numerical method could be another reason for the difference. It could be seen that the HCIS-NO_2 model agreed with the numerical solution of the ADE-NO_2 model.

The quantitative measures presented in Table 1 describes the coefficient of the Nash-Sutcliffe efficiency coefficient (NSE), root mean square error (RMSE), RMSE observation standard deviation ratio (RSR), and coefficient of determination (R^2), all of which were applied to assess the performance of the HCIS-NO_2 model. Figure 7 was used for the quantitative measures and it was observed from the table that the values of NSE and R^2 were closer to unity. Furthermore, the RMSE and RSR have a very small value. Consequently, the results of the quantitative measures signify an excellent correlation between both models.

Application of the Model to the Umgeni River

The efficiency of the proposed model was demonstrated by predicting the effect of nitrite concentration in Umgeni River. It is an important river situated in KwaZulu-Natal province of the Republic of South Africa, and it serves as a source of fresh water for the region. Agunbiade and Moodley (2014) described the river as having a drainage area of 4432km^2, with a length of approximately 232km. In addition, the river takes a mean annual precipitation of about 410-1450mm and an annual runoff of 72-680mm. However, the river has seen high levels of environmental degradation due to the many industries and agricultural operations situated close to the river discharging their waste effluents and agricultural runoff into the water body, thereby increasing the river's pollution level. The river reaches of 20km presented in Figure 8 from the Midmar Dam outflow (RMG003) to Morton's Drift (RMG008) was selected for this investigation. The observed data for nitrite concentration for the year 2014 were obtained from Umgeni River water. The daily precipitation data for the year 2014 was obtained from the Cedera station, which is about 19.5km from the first sampling point. The river flow details were obtained from South Africa's Department of Water and Sanitation. The actual flow data for sampling location RMG003 were used for the calibration of the HCIS-NO_2 model. The values of nitrite concentration for sampling location RMG003 were taken as the boundary condition for the model.

The data obtained for sampling point RMG003 were used to estimate the properties for the first reach. In addition, the properties obtained for the first reach were assumed to be used for the remaining reaches. The ammonia and nitrite oxidation rates were 0.002 per min and 0.005 per min, respectively. The reach length of 20km was separated into six reaches and each reach was further divided into several hybrid units with their own parameters. Table 2 describes the estimated model parameters, river geometry and hydraulic properties of the river.

Table 1: Correlation between ADE-NO_2 and HCIS-NO_2 models

Unit	R^2	RMSE	NSE	RSR
First	0.980	0.0028	0.972	0.0073
Second	0.964	0.0022	0.942	0.0082
Fourth	0.952	0.0025	0.931	0.0085
Eight	0.754	0.0034	0.711	0.0242

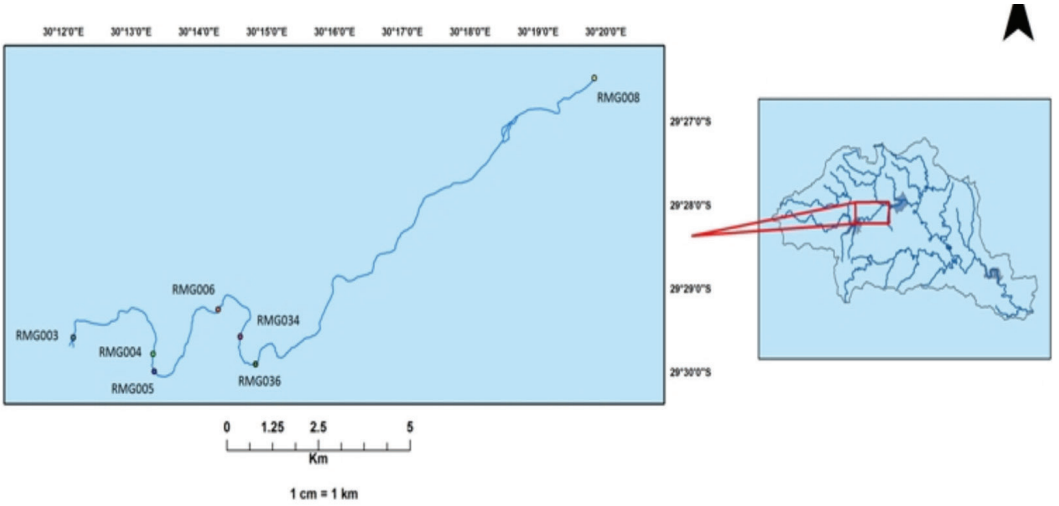

Figure 8: A map of Umgeni River with the sampling points

Table 2: Estimated model parameters and flow characteristics

	Reaches					
River properties/ HCIS model parameters	RMG003-RMG004	RMG004-RMG005	RMG005-RMG006	RMG006-RMG034	RMG034-RMG036	RMG036-RMG008
L (m) u (m/s	3200	950	2530	1650	960	11500
u (m/s	0.49	0.42	0.42	0.49	0.37	0.31
W (m)	6.0	7.4	7.0	6.0	8.2	9.4
H (m)	0.45	0.40	0.46	0.48	0.34	0.30
Q (m^3/s)	1.32	1.24	1.35	1.41	1.03	0.87
Avg. Slope	0.00335	0.0098	0.0084	0.0069	0.0037	0.0017
Δx (m)	344	351	373	411	308	302
T_1 (s)	187.32	190.96	202.92	223.48	167.58	164.28
T_2 (s)	234.43	238.70	253.65	279.36	209.48	205.35
T_3 (s)	515.11	525.15	558.03	614.59	460.87	451.78
Number of hybrid units	9	3	7	4	3	38

The hybrid model parameters (T_1, T_2, and T_3) were calculated as proposed in Ghosh (2001). The estimated longitudinal dispersion coefficient (D_L) and the size of the hybrid units (Dx) were used in calculating the model parameters. Etemad-Shahidi and Taghipour (2012) proposed an empirical equation to calculate the longitudinal dispersion coefficient after knowing the flow conditions and average river geometry of the water body, as presented in Eqs. (11 and 12). Hence, the proposed equation was applied to calibrate and determine the

D_L. In addition, the hybrid unit size (Dx) was determined by satisfying the Peclet number condition.

If W/ H ≤ 30.6,

$$D_L = 15.49\left(\frac{W}{H}\right)^{0.78}\left(\frac{u}{U_*}\right)^{0.11} * HU_* \quad (11)$$

Else

$$D_L = 14.12\left(\frac{W}{H}\right)^{0.61}\left(\frac{u}{U_*}\right)^{0.85} * HU_* \quad (12)$$

Where, W represents the width of the channel (m), H represents the depth of flow (m), U_* represents the shear flow velocity (m/s) and u is the mean flow velocity.

To perform the model simulation, the concentration of nitrite data for the first sampling location was applied as a step input into the model. Consequently, the predicted values of nitrite concentration downstream were compared with the measured data collected from Umgeni River water in 2014 as presented in Fig. 9(a)-(d). The figures demonstrate the comparison between the simulated and measured values of nitrite in Umgeni River between January and December 2014. The results illustrate that the general trends of the predicted dataset is in good agreement with the measured dataset for the period between January and March 2014. It was observed that the concentration of nitrite decreases in both measured and simulated profiles. Moreover, the reduction in nitrite concentration for the period was due to the low flow rate as presented in Fig. 9(e) and the influence of high temperature, which could

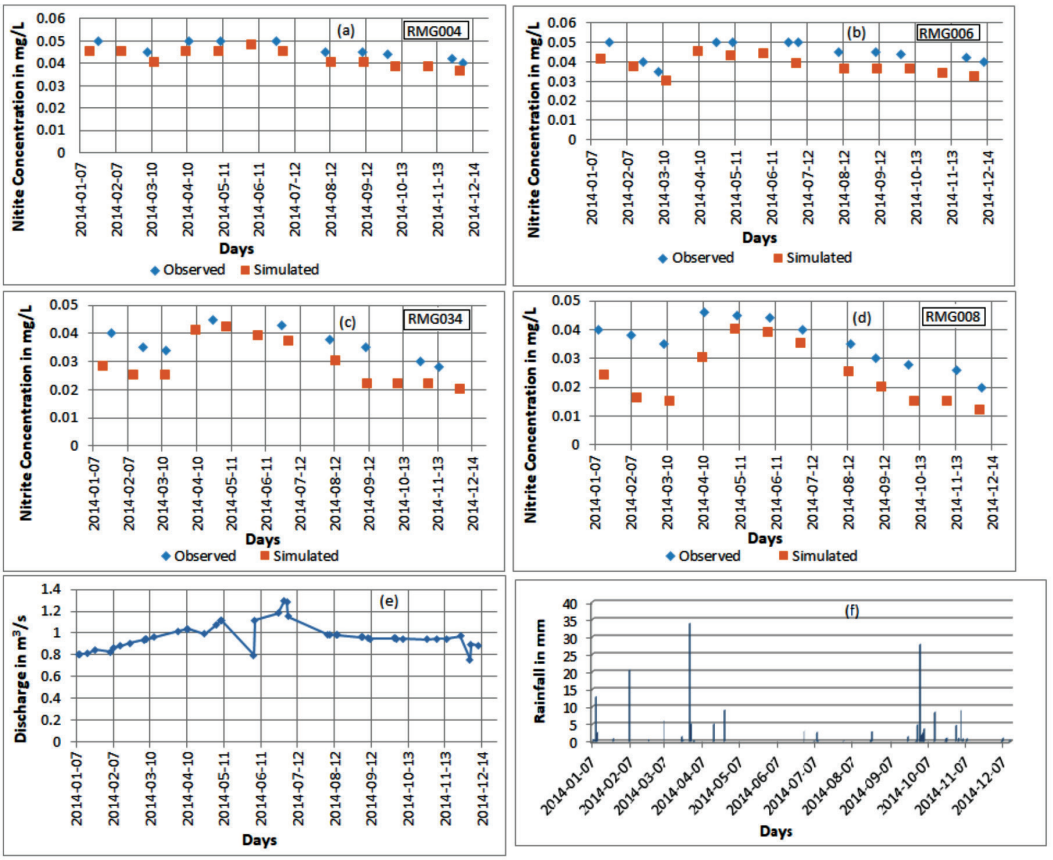

Figure S2: A comparison of the simulated and measured nitrite concentration at sampling locations RMG004 (a), RMG006 (b), RMG034 (c), and RMG008 (d), and in terms of average flow (e) and observed rainfall for the year 2014 (f)

be associated with the summer season. An increase in river temperature would intensify the activities of nitrifying bacteria, resulting in the formation of nitrate concentration in the water body through the nitrification process. Hence, the agreement between both sets of results could be deemed satisfactory. The trends of nitrite concentration for the period of between April and July were also compared and it was observed that there was an agreement between the measured and observed values. It could be seen from the figures that there was a significant increase in nitrite concentration for this period. The nitrite concentration increases as water flow increases, which indicates that the annual nitrite load is directly related to river flow. Therefore, the concentration of nitrate tends to increase during high intensive precipitation and high flow rate as supported. The increment in nitrite concentration for this period was because of high rainfall events as indicated in Fig 9(f). The high precipitation around this period tends to result in an increase of nutrient load into the river. In addition, the nitrite concentration for the period between August and December were also compared and a reduction in concentration of nitrite was observed in both profiles. The figures indicate a good agreement between the measured and observed profiles for this period. However, the discrepancy between the measured and simulated profiles for Fig 9(d) was due to a lack of data from Karkloof River, which joins sampling point RMG008. It can be concluded that the general trends of the model prediction agree with the measured datasets as observed from the figures.

To provide a more quantitative measure on the performance of the HCIS-NO_2 model, the model outputs were compared with the observed values. Statistical analysis in the form of coefficient of determination (R^2) and standard error (SE) were estimated for all the sampling locations as shown in Table 2. The results of the statistical measures presented in Table 3 indicate high R^2 values and low SE values, which shows that the model has a high significance in the simulation of nitrite concentration in the river. The R^2 and SE values, which were closer to unity and zero, respectively, show that the HCIS-NO_2 model closely reproduces the measured data.

Conclusions

This research presents the development and application of a hybrid model for the non-conservative transport of nitrite pollutant in a natural river. In this study, the advection-dispersion equation with a first-order kinetic reaction of nitrite was solved analytically using the concept of a hybrid model. The developed model was derived to predict the spatial and temporal variations of nitrite pollutant in a natural stream. The hybrid model consists of a plug flow cell and two unequal thoroughly mixed cells, all connected in series that have a single-timed model parameter per cell. The model parameters could be estimated with the flow velocity and longitudinal dispersion coefficient of the water body when the Peclet number condition is satisfied ($Pe \geq 4$). An analytical solution for the HCIS-NO_2 model was obtained in the plug flow cell and two thoroughly mixed cells using the principle of Laplace transformation. The simplicity of the HCIS model in solving an ordinary first-order differential equation and its flexibility to include additional reaction kinetics are advantages of the model. However, the new model does not consider the effect of lateral flow due to its restriction to non-rainy periods. This could be improved in the future by considering

Table 3: Correlation between measured and simulated values

River reach	R^2	SE
RMG 004	0.794	0.010
RMG 006	0.768	0.013
RMG 034	0.754	0.011
RMG 008	0.735	0.006

the effect of a non-point source pollution in its process. The usefulness of the new model was demonstrated with hypothetical data, where the unit step and the unit impulse response functions of the hybrid model were described. The performance of the HCIS-NO_2 model solution was verified through a comparison with the results of the Fickian-based ADE model. It was noticed that the response of the HCIS-NO_2 model with parameters (T_1, T_2 and T_3) almost matches the response of the ADE-NO_2 model with two parameters (u and D_L). Very high NSE and R^2 values were obtained in the statistical analysis, which indicates a good agreement between the HCIS-NO_2 model and the ADE-NO_2 model. The HCIS-NO_2 model was shown to be a valuable and successful tool for simulating solute transport in a natural river. The solution could be used to verify other models that are developed to simulate nitrite pollutant in natural steams.

Acknowledgements

The author duly acknowledges the support provided by the Water Research Commission of South Africa by funding this research through the project K5/2328.

References

Agunbiade, F. O., & Moodley, B. (2014). Pharmaceuticals as emerging organic contaminants in Umgeni River water system, KwaZulu-Natal, South Africa. *Environmental monitoring and assessment*, *186*(11), 7273-7291.

Banks, R. B. (1974). A mixing cell model for longitudinal dispersion in open channels. *Water Resources Research*, *10*, 357-358.

Balf, M. R., Noori, R., Berndtsson, R., Ghaemi, A., & Ghiasi, B. (2018). Evolutionary polynomial regression approach to predict longitudinal dispersion coefficient in rivers. *Journal of Water Supply*: *Research and Technology-Aqua, 67*(5), 447-457.

Bouraoui, F., & Grizzetti, B. (2014). Modelling mitigation options to reduce diffuse nitrogen water pollution from agriculture. *Science of the Total Environment*, *468*, 1267-1277.

Corriveau, J., Van Bochove E., Savard, M. M., Cluis, D., & Paradis, D. (2010). Occurrence of high in-stream nitrite levels in a temperate region agricultural watershed. *Water, Air, and Soil Pollution*, *206*(1-4), 335-347.

Etemad-Shahidi, A., & Taghipour, M. (2012). Predicting longitudinal dispersion coefficient in natural Streams using M5′ model tree. *Journal of Hydraulic Engineering*, *138*(6), 542-554.

Gavrilescu, M., Demnerová, K., Aamand, J., Agathos, S., & Fava F. (2015). Emerging pollutants in the environment: Present and future challenges in biomonitoring, ecological risks and bioremediation. *New biotechnology*, *32*(1), 147-156.

Ghosh, N. C. (2001). *Study of solute transport in a river*. Ph.D thesis, Dept of Civ. Eng., IIT. Roorkee, INDIA.

Ghosh, N. C., Mishra, G. C., & Kumarasamy, M. (2008). Hybrid-cells-in-series model for solute transport in streams and relation of its parameters with bulk flow characteristics. *Journal of Hydraulic Engineering*, *134*(4), 497-502.

Ghosh, N. C., Mishra, G. C., & Ojha, C. S. P. (2004). Hybrid-Cells-in-Series Model for solute transport in a river. *Journal of Environmental Engineering*, 1198-1209.

Kannel, P. R., Kanel, S. R., Lee, S., Lee, Y. S., & Gan T. Y. (2011). A review of public domain water quality models for simulating dissolved oxygen in rivers and streams. *Environmental Modeling & Assessment*, *16*, 183-204.

Kiedrzyńska, E., Kiedrzyński, M., Urbaniak, M., Magnuszewski, A., Skłodowski, M., Wyrwicka, A., & Zalewski, M. (2014). Point sources of nutrient pollution in the lowland river catchment in the context of

the Baltic Sea eutrophication. *Ecological Engineering*, *70*, 337-348.

Kumarasamy, M. (2015). Deoxygenation and reaeration coupled hybrid mixing cells based Pollutant Transport Model to assess water quality status of a river. *International Journal of Environmental Research*, *9*, 341-350.

Kumarasamy, M., Ghosh, N. C., Mishra, G. C., & Kansal, M. L. (2013). Hybrid model development for the decaying pollutant transport in streams. *International Journal of Environment and Waste Management*, *12*, 130-145.

Kumarasamy, M., Mishra, G. C., Ghosh, N. C., & Kansal, M. L. (2011). Semi analytical solution for non-equilibrium Sorption of Pollutant Transport in Streams. *Journal of Environmental Engineering*, *137,* 1066-1074.

Lewis, J. R., Wurtsbaugh, W. A., Paerl., & H. W. (2011). Rationale for control of anthropogenic nitrogen and phosphorus to reduce eutrophication of inland waters. *Environmental Science & Technology, 45,* 10300-10305.

Liu, S., Taylor, J. S., Randall, A., & Dietz, J. D. (2005). Nitrification modeling in chloraminated distribution systems. *Journal (American Water Works Association)*, *97*, 98-108.

Mirbagheri, S., Abaspour. M., & Zamani. K. (2009). Mathematical modeling of water quality in river systems. *European Water*, 31-41.

Neuman, S. P., & Tartakovsky D. M. (2009). Perspective on theories of non-Fickian transport in heterogeneous media. *Advances in Water Resources*, *32*(5), 670-680.

Nyenje, P. M., Foppen, J. W., Uhlenbrook, S., Kulabako, R., & Muwanga, A. (2010). Eutrophication and nutrient release in urban areas of sub-Saharan Africa - A review. *Science of the Total Environment*, *408*(3), 447-455.

Oliveira, B., Bola, J., Quinteiro, P., Nadais, H., Arroja, L. (2012). Application of Qual2Kw model as a tool for water quality management: Cértima River as a case study. *Environmental Monitoring and Assessment*, *184*(10), 6197-6210.

Olowe, K. O., & Kumarasamy, M. (2017). Development of the hybrid cells in series model to simulate ammonia nutrient pollutant transport along the Umgeni River. *Environmental Science and Pollution Research*, *24*(29), 22967-22979.

O'neil, J., Davis, T. W., Burford, M. A., & Gobler, C. (2012). The rise of harmful cyanobacteria blooms: the potential roles of eutrophication and climate change. *Harmful Algae*, *14*, 313-334.

Paredes, J., Andreu, J., & Solera, A. (2010). A decision support system for water quality issues in the Manzanares River (Madrid, Spain). *Science of the Total Environment*, *408*(12), 2576-2589.

Raimonet, M., Vilmin, L., Flipo, N., Rocher, V., & Laverman, A. M. (2015). Modelling the fate of nitrite in an urbanized river using experimentally obtained nitrifier growth parameters. *Water Research*, *73*, 373-387.

Sakalauskienė, G. (2001). Dissolved oxygen balance model for Neris. *Nonlinear Analysis, Modelling and Control*, *6*, 105-131.

Samatya, S., Kabay, N., Yüksel, Ü., Arda, M., & Yüksel, M. (2006). Removal of nitrate from aqueous solution by nitrate selective ion exchange resins. *Reactive and Functional Polymers*, *66*(11), 1206-1214.

Sattar, A. M., & Gharabaghi, B. (2015). Gene expression models for prediction of longitudinal dispersion coefficient in streams. *Journal of Hydrology, 524*, 587-596.

Seifi, A., & Riahi-Madvar, H. (2019). Improving one-dimensional pollution dispersion modeling in rivers using ANFIS and ANN-based GA optimized models. *Environmental*

Science and Pollution Research, 26(1), 867-885.

Seo, I. W., & Cheong, T. S. (1998). Predicting longitudinal dispersion co-efficient in natural streams. *J. of Hydraul. Eng., ASCE, 124*(1), 25-32.

Silva, M. A. M., Souza, M. F., & Abreu, P. C. (2015). Spatial and temporal variation of dissolved inorganic nutrients, and chlorophyll-α in a tropical estuary in northeastern Brazil: Dynamics of nutrient removal. *Brazilian Journal of Oceanography*, *63*(1), 1-15.

Smith, V. H., & Schindler, D. W. (2009). Eutrophication science: Where do we go from here? *Trends in Ecology & Evolution*, *24*(4), 201-207.

Wang, G. T., & Chen, S. (1996). A new model describing convective-dispersive phenomena derived by using the mixing-cell concept. *Applied Mathematical Modelling*, *20*(4), 309-320.

Wang, Q., Zhao, X., Yang, M., Zhao, Y., Liu, K., & Ma, Q. (2011). Water quality model establishment for middle and lower reaches of Hanshui River, China. *Chinese Geographical Science*, *21*(6), 646-655.

Varol, M., & Sen, B. (2012). Assessment of nutrient and heavy metal contamination in surface water and sediments of the upper Tigris River, Turkey. *Catena*, *92*, 1-10.

Vonder, Wiesche, M., & Wetzel, A. (1998). Temporal and spatial dynamics of nitrite accumulation in the River Lahn. *Water Research*, *32*(5), 1653-1661.

Yuceer, M., & Coskun, M. A. (2016). Modeling water quality in rivers: A case study of Beylerderesi River in Turkey. *Applied Ecology and Environmental Research*, *14*(1), 383-395.

Zamparas, M., & Zacharias, I. (2014). Restoration of eutrophic freshwater by managing internal nutrient loads. A review. *Science of the Total Environment*, *496*, 551-562.